Passivant dependence of nanoparticle-substrate interactions of alkanethiolate-passivated Au nanoparticles on graphite substrates

Imamura, Masaki

Tanaka, Akinori

(Citation)
Physical Review B,73(12):125409-125409

(Issue Date)
2006-03-13

(Resource Type)
journal article

(Version)
Version of Record

Passivant dependence of nanoparticle-substrate interactions of alkanethiolate-passivated Au nanoparticles on graphite substrates

Masaki Imamura*
Department of Physics, Graduate School of Science, Tohoku University, Aoba-ku, Sendai 980-8578, Japan

Akinori Tanaka†
Department of Mechanical Engineering, Faculty of Engineering, Kobe University, Nada-ku, Kobe 657-8501, Japan
(Received 7 October 2004; revised manuscript received 21 December 2005; published 13 March 2006)

We have carried out the photoemission study of monodisperse Au nanoparticles passivated with the various alkanethiolate on the highly oriented pyrolytic graphite (HOPG) substrate. The photoemission spectra in the vicinity of the Fermi level of alkanethiolate-passivated Au nanoparticles on the HOPG substrates are not the metallic Fermi edge. The steep slopes of Fermi level onsets move away from the Fermi level and depend on the surface-passivant molecules. We have analyzed the obtained spectra with the dynamic final state effect model that takes into account the Coulomb interaction between the photoelectron and photohole with a finite lifetime during the photoemission process. The calculated results based on the dynamic final state effect model reproduce the experimental ones fairly well. Furthermore, it is found that the photohole lifetime depends on the molecular length of surface-passivant. We attribute the passivant dependence of photoemission spectra to the surface-passivant dependent nanoparticle-substrate interaction.

DOI: 10.1103/PhysRevB.73.125409 PACS number(s): 73.22.−f, 73.90.+f

I. INTRODUCTION

Metallic nanoparticles have attracted much attention because of the potential applications such as biosensing, catalysts, and single-electron transistors.[1–3] Recently, metallic nanoparticles passivated with the organic molecules have been chemically synthesized.[4–6] These surface-passivated nanoparticles are self-assembled into a two- or three-dimensional nanostructure on a solid surface, and thus can easily manipulate the configuration with the surfactant and density. Furthermore, these nanoparticles are stable at room temperature and do not aggregate due to the existence of surface-passivants. From these properties, the molecule-passivated nanoparticles are suitable for future nanodevices. In order to develop the future nanodevice, the electron transfer between the nanoparticle and the substrate is considered to be a fundamental function, thus it is necessary to investigate the nanoparticle-substrate interaction. We have previously discussed nanoparticle-substrate interaction from the photoemission study of dodecanethiolate- (DT-) passivated Ag nanoparticles[7] synthesized with the two phase method.[8] The photoemission spectra in the vicinity of the Fermi level of DT-passivated Ag nanoparticles are not the metallic Fermi edge. The steep slopes of the Fermi level onsets move away from the Fermi level and show the size dependence. We have concluded in a previous report that this spectral feature in the vicinity of the Fermi level is due to the final state effect in photoemission, indicative of the interaction between the nanoparticle and substrate through the surface passivants on a femtosecond time scale. However, in the previous experiment, the observed photoemission spectra included the inhomogeneous width due to the size distribution, which prevented obtaining the homogeneous spectrum. In order to discuss the size-dependent spectrum, we need to prepare the monodisperse sample. Additionally, there is no report about the dynamic final-state effect as a function of the passivant molecular length, that is, the passivant dependence of nanoparticle-substrate interaction.

In this paper, we report the results of the passivant dependent photoemission studies of the alkanethiolate- (AT-) passivated Au nanoparticles on the highly oriented pyrolytic graphite (HOPG) substrate. In order to obtain the intrinsic spectrum, we prepared the monodisperse AT-passivated Au nanoparticles by the digestive-ripening process.[9,10] Furthermore, in order to investigate the passivant dependence, we prepared the Au nanoparticles passivated with the various alkanethiol [octanethiol (OT), DT, hexadecanethiol (HDT)] that have different molecular lengths. From these experiments, we will discuss the passivant dependence of the nanoparticle-substrate interaction.

II. EXPERIMENT

The series of AT-passivated Au nanoparticles were synthesized with a method developed by Lin *et al.*[9,10] First, the didodecyldimethylammonium bromide (DDAB) was added to toluene and distilled water to form the micelle solution. Gold chloride was dissolved to this micelle solution by sonication. An aqueous sodium borohydride was added with stirring, and then Au nanoparticles were obtained. While stirring, alkanethiol [OT ($C_8H_{17}SH$), DT ($C_{12}H_{25}SH$), HDT ($C_{16}H_{33}SH$)] was added to ligate the Au surface through the ligand exchange. After that, Au nanoparticles were precipitated with ethanol, evaporated, and redissolved into toluene. Another alkanethiol (OT, DT, HDT) was added, and the nanoparticle solution was heated. The annealed nanoparticle solution was diluted by boiled toluene and left 1 day. This procedure induced the size segregation during the slow lowering of the nanoparticle temperature. The top layer of this nanoparticle solution was separated, evaporated, and washed

with ethanol repeatedly to remove excess thiol. The precipitates were finally dissolved to toluene. Then highly monodisperse AT-passivated Au nanoparticle were obtained. The size of obtained AT-passivated Au nanoparticles was controlled by the ratio of water and DDAB. The size distribution in the diameter and shape of the AT-passivated Au nanoparticles were observed by transmission electron microscopy (TEM). Additionally, we performed the optical extinction measurements. For the photoemission measurements, the synthesized AT-passivated Au nanoparticles were supported on the HOPG substrates by evaporating the solvent (toluene) from the dispersion of AT-passivated Au nanoparticles on the single-crystalline HOPG cleaved surface in a nitrogen-filled glove bag directly connected to the ultrahigh-vacuum photoelectron spectrometer. Then the samples were transferred into the photoemission analysis chamber without exposure to air. The cleanliness was checked by *in situ* Auger electron spectroscopy (AES). The prepared samples show no AES signals from the contaminants. The photoemission measurements were performed at 40 K with He I resonance line as an excitation source.

III. RESULTS AND DISCUSSION

Figure 1 shows the TEM images and size distributions for the present AT-passivated Au nanoparticles used in this work. The size distributions were determined from several TEM micrographs of the corresponding samples. The obtained mean diameters from TEM observation are 4.2, 4.1, and 3.8 nm for the surface passivants of OT, DT, and HDT, respectively. The standard deviations are 0.28, 0.38, and 0.4 nm for the surface passivants of OT, DT, and HDT, respectively. From the obtained TEM images, the present AT-passivated Au nanoparticles show the homogeneous and spherical shape, and each nanoparticle separates from the neighboring nanoparticles, indicating that present Au nanoparticles are well-passivated by the alkanethiol molecules. The standard deviations of the present nanoparticles are less than about 10%. The present Au nanoparticle samples have narrower size distribution than previous DT-Ag nanoparticles synthesized by the two phase method.

Figure 2 shows the photoemission spectra in the vicinity of Fermi level of the present AT-passivated Au nanoparticles and bulk Au. The spectrum of bulk Au has the metallic Fermi edge, with the midpoint of the steep slope just at the Fermi level. However, the leading edges of the spectra in the vicinity of the Fermi level of all the AT-passivated Au nanoparticles moved away from the Fermi level. Furthermore, an important point to note is that the slopes of the leading edges depend on the surface passivants. The slopes of the leading edges become steep with decreasing the molecular length of the surface-passivant. In our previous work, we have reported that the photoemission spectra in the vicinity of the Fermi level of DT-passivated Ag nanoparticles show the deviation from the metallic Fermi edge, and these spectra reflect the final-state effect.[7] We have explained the experimental spectra using a theoretical model that takes into account the influence of the photohole remaining on the nanoparticle during the photoemission process and the nanoparticle-

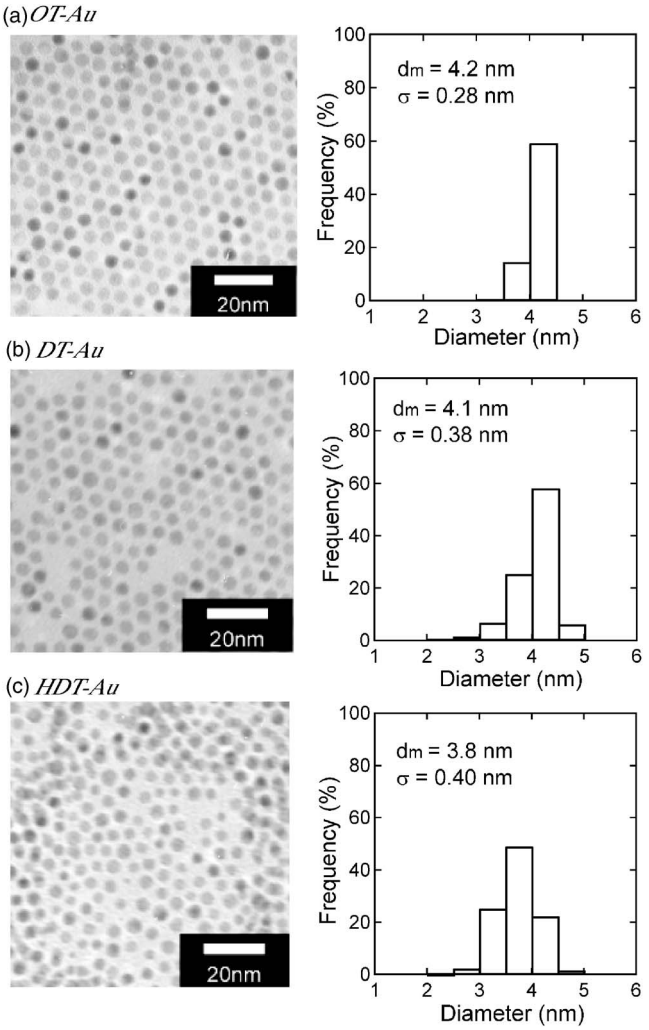

FIG. 1. TEM micrographs and size distributions in AT-passivated Au nanoparticles with mean diameters d_m and standard deviations σ.

substrate interaction. The present photoemission spectra have the same tendency as previous photoemission ones of DT-passivated Ag nanoparticles, therefore the present spectra would be explained by the same picture as described below. In general, a photoemission spectrum is attributed to the initial-state effect that directly reflects the sample electronic state, and also to the final-state effect that originates from the photohole created by the photonization. Therefore the present photoemission spectra seem to indicate that the AT-passivated Au nanoparticles exhibit nonmetalic electronic structures. Figure 3 shows the optical extinction spectra of the present AT-passivated Au nanoparticles in dilute toluene solution. As shown in Fig. 3, present nanoparticle samples show the distinct Mie plasmon resonance, indicating the collective motion of valence electrons typical for a metallic material. Thus present nanoparticle samples are considered for keeping the metallic electronic structure. Furthermore, from Kubo criterion, this discussion was reasonable for this size region of the present samples.[11] Thus the electronic structures of present nanoparticle samples are considered to be metallic ones. This discussion means that the spectral shapes

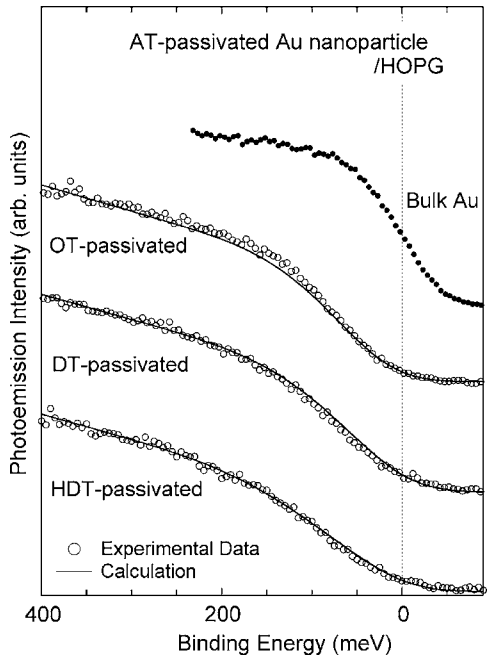

FIG. 2. The optical extinction spectra of present AT-passivated Au nanoparticles measured in toluene solution. Surface-passivants are indicated on each spectra.

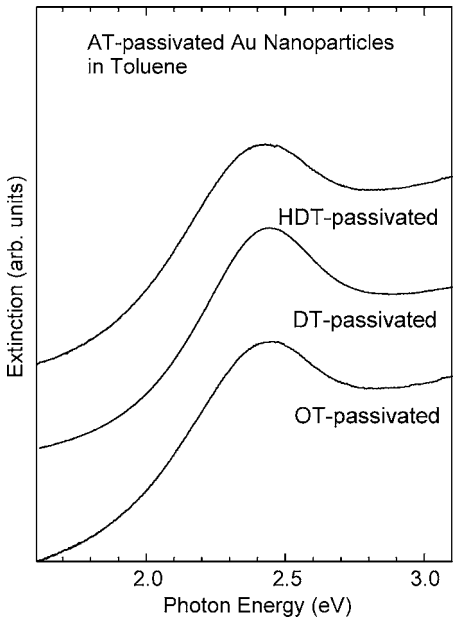

FIG. 3. The photoemission spectra in the vicinity of Fermi level of AT-passivated Au nanoparticles supported on HOPG substrates at 40 K measured with the He I resonance line (21.2 eV). Surface-passivant is indicated on each spectrum. Open circles and solid lines show the experimental photoemission spectra and the fits to the experimental spectra, respectively. The top spectrum shows the Fermi level onset observed for bulk Au polycrystalline evaporated film for a comparison.

of AT-passivated Au nanoparticles are attributed not to initial-state effect reflecting the change in electronic structure. Therefore these specific spectral features in the vicinity of the Fermi level of the present AT-passivated Au nanoparticles originate from the final-state effect due to the photohole left behind in the nanoparticles during the photoemission process. In this experiment, the nanoparticles are passivated with molecules, therefore the photohole left behind in the nanoparticles is not neutralized immediately. Thus the photohole left behind in the nanoparticles during the time scale relevant to the photoemission process will lower the kinetic energy of photoelectrons through the Coulomb interaction. In fact, these final-state effects on the core-level photoemission spectra have been reported for the free nanoparticles[12] and even for the nanoparticles on the substrates.[13] The final-state effect would play a more important role in the present surface-passivated Au nanoparticles, since the AT-passivated Au nanoparticles are weakly coupled with the HOPG substrate. From the static view, the kinetic energy shift of photoelectrons due to the photohole left behind in the nanoparticle is given by $\Delta E = e^2/2C = 1/2(e^2/4\pi\varepsilon_0 R_N)$, where $C = 4\pi\varepsilon_0 R_N$ is the self-capacitance of the nanoparticle with a radius of nanoparticle R_N. On the other hand, an exact calculation shows that the energy shift is given by $\Delta E = \alpha e^2/4\pi\varepsilon_0 R_N$, where α is the deviation from the values from 1/2, which depends on the material via the Wigner-Seitz radius. Seidl has reported that the value of α in the silver is 0.41 from the measurements of the ionization potentials. It is previously reported that Wigner-Seitz radii of Ag and Au are 3.02 and 3.01, respectively.[14] Therefore the value of Au is 0.41, which is almost same as Ag. In order to theoretically describe this observation, we use the dynamic final-state effect model[13,15,16] that takes into account the Coulomb interaction between the photoelectron and photohole with a *finite lifetime* during the photoemission process, as we carried out previously. In this model, the neutralization probability of the photohole during the time interval $[t, t+dt]$ is given by $P(t)dt = (1/\tau)\exp(-t/\tau)dt$ with the characteristic time τ. This characteristic time τ corresponds to the *finite lifetime* determined by the nanoparticle-substrate coupling strength, and interpreted as a tunneling time in the case of a weak nanoparticle-substrate interaction. While remaining the photohole, the Coulomb interaction between the photoelectron and the photohole reduce the kinetic energy. The Coulomb potential acting on the photoelectron due to the photohole is given by $W(r) = \alpha e^2/4\pi\varepsilon_0(1/R - 1/r)$, where r is the distance from the center of the nanoparticle. When the photohole neutralized after time t, the energy shift for the photoelectron is expressed with velocity of photoelectron v as $W(R_N + vt)$. The obtained spectra are averaged over a large number of photoelectrons at the different time t, therefore this leads to a distribution of energy shift given by

$$P(W)dW = \frac{C_N W_{\max}}{(W_{\max} - W)^2} \exp\left(-\frac{C_N W}{W_{\max} - W}\right) dW, \qquad (1)$$

with $C_N = R_N/vt$ and $W_{\max}$, $W_{\max}$ corresponds to the maximum energy shift. In the case of photoemission in the vicinity of Fermi level for the nanoparticle, the intrinsic photoemission spectral features $S(E_B, R_N)$ can be described by the convolution of Fermi-Dirac distribution at relevant temperature and energy-shift distribution function $P(W)$ in Eq. (1),

as a function of binding energy E_B. In addition to the intrinsic spectral feature $S(E_B,R_N)$, the experimental photoemission spectra include the contribution from the inhomogeneous width due to the size distribution as shown in Fig. 1, since the photoemission spectrum $S(E_B,R_N)$ depends on a nanoparticle radius R_N. Furthermore, the observed photoemission spectra in the present experiments also include the contributions from the finite instrumental function and the photoemission intensity from the uncovered region of HOPG substrate. Thus the observed spectra $I(E_B)$ in the present experiments are expresed by

$$I(E_B) \propto [S(E_B,R_N) \otimes D(R_N)] \otimes G(E_B) + B(E_B), \qquad (2)$$

where $D(R_N)$ is a Gaussian size distribution function in radius determined from the TEM observation, $B(E_B)$ is the photoemission intensity from the HOPG substrate determined by the experimental spectrum of HOPG, and $G(E_B)$ is an instrumental Gaussian function derived from a fit to experimental Fermi edge of bulk Au. The solid line in Fig. 2 shows the calculated spectrum by the dynamic final-state effect model. As shown in Fig. 2, the fitting results reproduce the experimental spectra of all AT-passivated samples fairly well. The obtained photohole lifetime τ from the calculations are 0.27×10^{-15}, 0.32×10^{-15}, and 0.41×10^{-15} s for the surface passivants of OT, DT, and HDT, respectively. It is concluded that the observed spectral features for all the AT-passivated Au nanoparticles on the HOPG can be explained with the dynamic final-state effect model and reflect the nanoparticle-substrate interactions through the surface passivants on a femtosecond time scale. Furthermore, it is found that the obtained photohole lifetime τ of each AT-passivated Au nanoparticle depends on the surface-passivants. The photohole lifetime τ increase with increasing of the molecular length of surface-passivants. In this system, surface-passivants length that corresponds to the separation between the nanoparticles and substrate determines the coupling strength. The photoemission spectra reflect the coupling strength between the nanoparticles and substrate. Therefore passivants dependent photoemission spectra reflect the coupling strength that depends on the nanoparticle-substrate interaction. In order to quantitatively analyze the passivant dependence of the lifetime τ, we plot in Fig. 4 the lifetime τ as a function of the half of the mean interparticle distance determined from the TEM micrographs. The mean interparticle distance is determined from the interparticle distance distribution within the close-packed array regions, which is considered to be an intrinsic interparticle separation. Half of the interparticle distance corresponds to intrinsic nanoparticle-substrate separation. The solid line is a fitting line to the experimental data by the least-squares method. This analysis shows that these lifetimes exponentially depend on the half of the interparticle distance between nanoparticles and the substrate. In other words, the lifetime τ exponentially depends on the separation between the nanoparticles and substrate. On the other hand, the lifetimes τ of the photohole directly correspond to the tunneling times through the surface-passivants. From the analogy of the single electron tunneling, these photohole lifetimes τ can be estimated to $\tau = RC$, where R is the tunneling resistance between the nanoparticle and substrate through the passivants, and C is the self-capacitance of the nanoparticle. The mean diameters among the present nanoparticles are almost the same, thus it is considered that the self-capacitance of each nanoparticle sample is almost the same. Therefore the passivant dependence of the tunneling time τ is arised from the difference of the dependence of the tunneling resistance R between nanoparticles and substrate among the present samples. The tunneling resistance R is expressed as $R \propto \exp(\beta x)$, β is the decay constant, x corresponds to the distance between Au nanoparticles and substrate in this experiment. Thus it is concluded that the dependence of the tunneling time τ on the half of interparticle distance (as shown in Fig. 4) corresponds to the dependence of the tunneling resistance on the tunneling gap width. This result indicates that the photoemission spectrum of the AT-passivated Au nanoparticle supported on the HOPG substrate reflects the electron tunneling through the surface passivants. Through the observation of the final-state effect in the photoemission spectra, we provide the knowledge about the electron transfer phenomenon in the metal-molecule-metal.

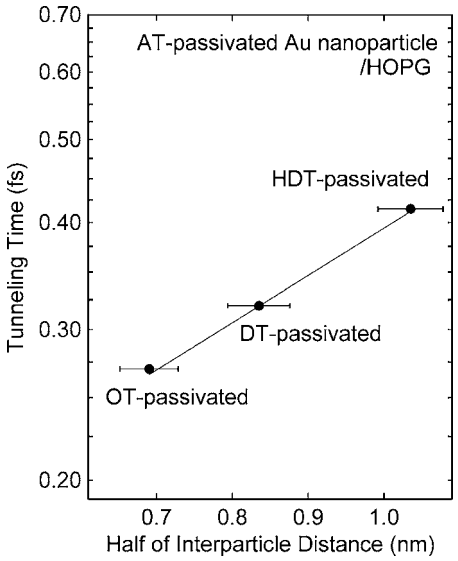

FIG. 4. A semilog plot of the tunneling time τ as a function of the half of interparticle distance. Points and solid line show the tunneling time τ and the fits to the tunneling time τ by the least-squares method. Error bars are standard deviation of the half of interparticle distance.

IV. CONCLUSION

In this contribution, we have investigated the passivant dependence of nanoparticle-substrate interaction on the series of chemically synthesized AT-passivated Au nanoparticles using the photoemission spectra in the vicinity of the Fermi level. It is found that the leading edges of the photoemission spectra show the distinct spectral feature, with the midpoints of the steep slopes moved away from the Fermi level. These spectra were reproduced with the dynamic final-state effect model taking into account the influence of the

photohole remaining on the nanoparticle after the photoemission process. The obtained lifetimes τ by fitting with the dynamic final-state effect model depend on the surface-passivants. From the analysis, it is found that the obtained photohole lifetimes τ exponentially depend on the molecule length of surface-passivants. It is concluded that the dependence of the tunneling time τ on the half of interparticle distance corresponds to the dependence of the tunneling resistance on the tunneling gap width.

ACKNOWLEDGMENTS

We thank H. Sasaki and Y. Takeda of Department of Physics, Tohoku University, and A. Yamaguchi of Department of Chemistry, Tohoku University for help in the experiments. This work was supported by a grant from the Ministry of Education, Culture, Sports, Science and Technology of Japan.

*Electronic address: masaki@mail.tains.tohoku.ac.jp
†Author to whom correspondence should be addressed. Electronic address: a-tanaka@mech.kobe-u.ac.jp

[1] C. A. Mirkin, R. L. Letsinger, R. C. Mucic, and J. J. Storhoff, Nature (London) **382**, 607 (1996).
[2] M. P. A. Viegers and J. M. Trooster, Phys. Rev. B **15**, 72 (1977).
[3] T. Sato, H. Ahmed, D. Brown, and B. F. G. Johnson, J. Appl. Phys. **82**, 696 (1996).
[4] R. M. Crooks, M. Zao, L. Sun, V. Chechik, and L. K. Yeung, Acc. Chem. Res. **34**, 181 (2001).
[5] D. Gerion, N. Zaitseva, C. Saw, M. F. Casula, S. Fakra, T. Van Buuren, and G. Galli, Nano Lett. **4**, 597 (2004).
[6] J. Zheng, C. Zhang, and R. M. Dickson, Phys. Rev. Lett. **93**, 077402 (2004).
[7] A. Tanaka, Y. Takeda, T. Nagasawa, and S. Sato, Phys. Rev. B **67**, 033101 (2003).
[8] M. Brust, M. Walker, D. Bethell, D. J. Schiffrin, and R. Whyman, J. Chem. Soc., Chem. Commun. **1994**, 801.
[9] X. M. Lin, C. M. Sorensen, and K. J. Klabunde, J. Nanopart. Res. **2**, 157 (2000).
[10] X. M. Lin, H. M. Jaeger, C. M. Sorensen, and K. J. Klabunde, J. Phys. Chem. B **105**, 3353 (2001).
[11] R. Kubo, A. Kawabata, and S. Kobayashi, Annu. Rev. Mater. Sci. **14**, 49 (1984).
[12] M. Seidl, K.-H. Meiwes-Broer, and M. Brack, J. Chem. Phys. **95**, 1295 (1991).
[13] A. Tanaka, Y. Takeda, M. Imamura, and S. Sato, Phys. Rev. B **68**, 195415 (2003).
[14] N. W. Ashcroft and N. D. Mermin, *Solid State Physics* (Sanders College, Philadelphia, 1976).
[15] H. Hövel, B. Grimm, M. Pollmann, and B. Reihl, Phys. Rev. Lett. **81**, 4608 (1998).
[16] H. Hövel, I. Barke, H. G. Boyen, P. Ziemann, M. G. Garnier, and P. Oelhafen, Phys. Rev. B **70**, 045424 (2004).